APPLICATION OF RFSP-IST DETERMINED TRIP DELAY TIME TO WOLSONG-1 LOSS OF REGULATION SIMULATIONS

Dai-Hai Chung[1*], Jong-Hyun Kim[1], Cheon-Hwey Cho[1] and Sung-Min Kim[2]
[1]Atomic Creative Technology Co., Ltd., Daejeon, Korea
[2]Korea Hydro and Nuclear Power Co., Ltd., Daejeon, Korea
[*]*Corresponding author: dhchung@actbest.com*

Abstract

The trip delay time that is determined by using RFSP-IST is applied to the Loss of Regulation (LOR) simulations of Wolsong-1, which is scheduled to undergo a major refurbishment project. The safety analyses required for licensing after refurbishment are currently being carried out using the update-to-date Canadian Industry Standard Toolset code suite. Since the POINTSIM program used in the past to calculate trip delay time is not included in IST, the RFSP-IST code is being mandatorily used in place of the POINTSIM functions. The CATHENA LOR simulation results obtained based upon the RFSP-IST determined trip delay times clearly justify the use of procedures that are developed to run *CERBERUS, *INTREP and *TRIP_TIME modules in the context of determining trip delay time.

1. Introduction

The Wolsong NPP Unit 1 (Wolsong-1) is being prepared with the safety analysis work for the restart of the reactor after the major refurbishment project. These analyses are being carried out using the up-to-date Canadian Industry Standard Toolset code suite. For the Loss of Regulation (LOR) – Loss of Reactivity Control – analysis, CATHENA (Ref. 1) is used.

In order to run the CATHENA code for the simulation of LOR, the trip delay time of SDS1/2 – shutdown system – high neutron power trip (ROP – Regional Overpower Protection) and high rate-log trip is required as input to the code so that the point kinetics neutronic model of CATHENA can determine the appropriate trip time followed by the shutoff rods negative reactivity insertion, which in turn affects the shape of power transient and the final status of the fuel element sheath temperature. For the LOR analyses of Wolsong-2/3/4 (Refs. 2-3), the code system POINTSIM/SOPHT (Refs. 4-5) was used to calculate trip delay time as well as to examine the accident related relevant parameters after LOR.

The POINTSIM code is no longer supported, and, therefore, not included in the IST code suite. However, *TRIP_TIME module of RFSP-IST (Ref. 6) is now equipped with the previous important POINTSIM functions that include the trip delay time characteristics, so that the trip time corresponding to the actuation of the shutdown system can be obtained by running the module. But the module does not offer trip delay time. Thus, it has been locally decided to use *CERBERUS, *INTREP and *TRIP_TIME modules of RFSP-IST to simulate separately only the neutronic part of LOR transient beforehand, and subsequently to determine the trip activation (initiation) time for a given trip setpoint from the fine shape of detector flux transients. Finally, the trip delay time can then be determined by subtracting the trip activation (initiation) time from the SDS1/2 actuation trip time that is explicitly shown in the RFSP-IST output.

In the following, the procedures developed to determine trip delay time using RFSP-IST will be explained, and the so obtained trip delay times will be compared with the previously POINTSIM calculated trip delay times (Refs. 3-4). Furthermore, the CATHENA LOR simulation results obtained for a simple case based upon the RFSP-IST and POINTSIM calculated trip delay times are presented and discussed followed by some conclusions.

2. Wolsong-1 Refurbished Fresh Core Model

The reactor physics model of Wolsong-1 refurbished core is set up using WIMS-IST (Ref. 7) and RFSP-IST code systems. The WIMS-IST code produces the base data of lattice physics parameters that are further used to generate the relevant reactor physics data, such as, the macroscopic fuel properties (Ref. 8), which are required by RFSP-IST to produce the global flux and power distribution in the core. The presence and effects of the various reactivity devices in the core are represented by the incremental cross sections that are calculated by the WIMS-IST/T16MAC/DRAGON-IST code system (Ref. 9-10).

TOTAL REACTOR POWER = 2061.40 MW
TOTAL FISSION POWER = 2156.01 MW
MAXIMUM CHANNEL POWER DIFFERENCE = 5.957 (%), 370 (kW) LOCATION IS CHANNEL M-12

	1	2	3	4	5	6	7	8	9	10	11	12	13	14	15	16	17	18	19	20	21	22
A									-3.93	-3.97	-3.98	-3.96	-3.97	-3.93								
B						-3.82	-3.79	-3.74	-3.66	-3.63	-3.63	-3.63	-3.65	-3.69	-3.70	-3.80	-3.82					
C					-3.73	-3.61	-3.45	-3.29	-3.16	-3.07	-3.02	-3.02	-3.05	-3.16	-3.29	-3.43	-3.61	-3.71				
D				-3.67	-3.47	-3.22	-2.89	-2.60	-2.36	-2.19	-2.12	-2.10	-2.18	-2.34	-2.59	-2.87	-3.21	-3.45	-3.68			
E			-3.64	-3.47	-3.09	-2.60	-2.05	-1.56	-1.13	-0.88	-0.77	-0.77	-0.86	-1.14	-1.54	-2.03	-2.59	-3.07	-3.46	-3.63		
F			-3.48	-3.19	-2.64	-1.91	-0.95	-0.20	0.50	0.92	0.98	0.99	0.91	0.52	-0.18	-0.93	-1.90	-2.63	-3.17	-3.47		
G		-3.52	-3.28	-2.85	-2.12	-1.17	0.03	1.01	1.89	2.39	2.48	2.50	2.41	1.89	1.03	0.05	-1.15	-2.12	-2.82	-3.27	-3.53	
H		-3.43	-3.06	-2.46	-1.57	-0.42	0.97	2.09	3.04	3.59	3.72	3.70	3.60	3.04	2.11	0.99	-0.41	-1.56	-2.45	-3.05	-3.41	
J	-3.51	-3.26	-2.80	-2.07	-0.94	0.37	1.95	3.12	3.99	4.51	4.67	4.68	4.51	3.97	3.12	1.94	0.39	-0.93	-2.02	-2.77	-3.26	-3.50
K	-3.42	-3.11	-2.55	-1.65	-0.19	1.25	2.69	3.86	4.70	5.24	5.40	5.42	5.24	4.70	3.87	2.70	1.27	-0.17	-1.64	-2.52	-3.11	-3.41
L	-3.36	-3.00	-2.37	-1.38	0.20	1.65	3.08	4.24	5.10	5.65	5.84	5.86	5.65	5.10	4.25	3.09	1.67	0.23	-1.37	-2.36	-2.98	-3.34
M	-3.30	-2.93	-2.28	-1.30	0.30	1.73	3.16	4.34	5.19	5.77	5.96	5.96	5.77	5.22	4.35	3.16	1.75	0.30	-1.27	-2.27	-2.92	-3.28
N	-3.24	-2.93	-2.31	-1.40	0.06	1.45	2.89	4.12	4.99	5.57	5.74	5.74	5.55	5.01	4.12	2.91	1.46	0.08	-1.37	-2.30	-2.91	-3.25
O	-3.21	-2.95	-2.42	-1.64	-0.48	0.80	2.39	3.63	4.53	5.11	5.27	5.27	5.11	4.55	3.65	2.41	0.81	-0.47	-1.62	-2.40	-2.92	-3.18
P		-2.96	-2.56	-1.92	-0.96	0.22	1.65	2.81	3.79	4.36	4.50	4.49	4.38	3.81	2.81	1.66	0.24	-0.93	-1.89	-2.54	-2.96	
Q		-2.99	-2.70	-2.17	-1.38	-0.34	0.91	1.94	2.85	3.37	3.48	3.47	3.37	2.85	1.94	0.93	-0.34	-1.36	-2.17	-2.68	-2.97	
R			-2.81	-2.40	-1.77	-0.94	0.09	0.87	1.62	2.04	2.13	2.13	2.04	1.64	0.89	0.10	-0.94	-1.76	-2.38	-2.79		
S			-2.86	-2.62	-2.17	-1.58	-0.95	-0.39	0.05	0.33	0.46	0.47	0.35	0.05	-0.39	-0.93	-1.56	-2.15	-2.59	-2.84		
T				-2.75	-2.43	-2.07	-1.68	-1.32	-1.03	-0.86	-0.78	-0.76	-0.86	-1.03	-1.32	-1.68	-2.05	-2.46	-2.75			
U					-2.64	-2.45	-2.19	-1.96	-1.81	-1.68	-1.65	-1.63	-1.68	-1.79	-1.96	-2.19	-2.42	-2.64				
V						-2.63	-2.50	-2.37	-2.30	-2.24	-2.23	-2.23	-2.26	-2.28	-2.37	-2.50	-2.59					
W									-4.83	-2.54	-2.54	-2.54	-2.57	-2.53								

Figure 1 Relative Differences between Time-Average Channel Powers with Depleted and Undepleted Adjuster Rod Loading (Rel. Diff (%)=[Depl./Undepl.-1]x100)

For the modelling of the reactivity devices, a significant change has been introduced to the Wolsong-1 core model in order to take account for the depletion of the stainless steel adjuster rods. The results of a separate study conducted to assess the effect of adjuster rod depletion are presented elsewhere (Ref. 11). In the present paper, the incremental cross sections of both the depleted and undepleted adjuster rods are used for comparison purposes. The relative differences between the time-average channel power distributions for the case of depleted and undepleted adjuster rod loading are shown in Figure 1.

The results are based upon the same time-average exit irradiation of each burnup zone. The maximum channel power for the depleted and undepleted cases are 6838.38 kW (th) at location J-11 and 6653.95 kW (th) at location H-08, respectively. The maximum channel power itself is increased by 184.43 kW (th), although the most increased value is 370 kW (th) (5.957%) at location M-12. It

is clearly seen that the inner 220 channels in the central region of the core show consistently the increase of channel power due to the depletion effect of adjuster rods, whereas the rest of the other 160 channels in the outer region display the opposite. These phenomena are also reflected in the feed rate of fresh fuel bundles and, e.g., in the inner central region the depletion effect of adjuster rods results in the increase of feed rate corresponding approximately to ~0.12 bundles/FPD and vice versa in the outer region.

The fresh core model loaded with two depleted fuel bundles at the bundle positions 8 and 9 in the central 80 channels is used for the present study. The boron concentrations in the moderator system are 2.747 ppm and 2.606 ppm for the depleted and undepleted adjuster rod loading cases, respectively. The SCM (Refs. 7, 8 and 12) fuel properties are used for the RFSP-IST simulations.

3. Procedure of RFSP-IST Trip Delay Time Determination

The procedures developed in the present study to determine trip delay time are explained here. As already mentioned in Section 1, three modules of RFSP-IST are involved, namely, *CERBERUS, *INTREP and *TRIP_TIME modules.

3.1 LOR Reactivity Insertion Rate

The simulation of LOR using CATHENA is modelled by inserting reactivity worth into the core with constant insertion rate (mk/s) for the given initial reactor power level. The CATHENA code then integrates the point model time-dependent reactor kinetics equations to simulate the total power transient.

In order to make the LOR reactivity insertion rate comparable with the CATHENA input, the LOR reactivity insertion in RFSP-IST is modeled by decreasing the coolant density with constant rate, i.e., linear change in time uniformly with a constant fractional decrease at all the fuel bundle positions in the core. The amount of coolant density decrease is determined according to the prescribed constant reactivity insertion rate as it would be input to CATHENA. The LOR transient is then simulated using *CERBERUS module, which gives the dynamic reactivity worth at each time point.

The amount of the coolant density decrease is iteratively adjusted in such a way that the time-dependent reactivity increase rate calculated by *CERBERUS module would be on average close to the constant reactivity insertion rate. In other words, the trip delay times so determined by RFSP-IST could be directly comparable with the trip delay times calculated by the POINTSIM program in the past.

The coolant density distribution at each bundle position in the core to be used for *CERBERUS module –TH GROUPS trailer card - is generated by using GENHTP module of CATHENA.

3.2 Trip Activation (Initiation) Time

The flux transients at 34 SDS1-SIR and 24 SDS2-SIR detector sites as well as 6 SDS1-IC and 6 SDS2-IC ion chambers are derived using *INTREP module from the flux shape transients stored in Direct Access File (DAF) of RFSP-IST. These detector and ion chamber fluxes are then processed

in an independent of RFSP-IST written Fortran program, and interpolated with fourth order polynomials using the method given in Reference 13, for time step sizes $\Delta t \leq 1$ ms. The numerical values of detector flux level and rate-log at each detector site and ion chamber, respectively, are monitored as the flux interpolation at the corresponding locations progresses in time until the very first one of the interpolated values hits the trip setpoint of the corresponding detector and ion chamber group. Then the time point at which this occurs is taken as the trip activation (initiation) time. Crediting only the very first hit of the trip setpoint would result in a conservative estimate of trip delay time.

The current Wolsong-1 safety analysis applied trip setpoints are 1.162 for SDS1/2 high neutron power trip (ROP), and 0.108 and 0.173 for SDS1 and SDS2 high rate-log trips, respectively

3.3 Shutdown System Actuation Trip Time

The trip time at which the shutdown system is actually actuated is directly obtained from *TRIP_TIME module that uses the flux shape transients at each detector site as well as ion chamber. The input to *TRIP_TIME module is directly imported from Reference 4. As for the case of trip activation (initiation) time determination, fourth order polynomial interpolation is used for the interpolation of transient flux shapes at detector sites and ion chambers in *TRIP_TIME module.

4. Results of Trip Delay Time Determination

The trip delay times determined by using RFSP-IST with the depleted adjuster rod loading are shown in Table 1 along with the trip delay times calculated by POINTSIM for 100% FP initial power level for the fresh core. The shutdown system actuation trip times calculated by RFSP-IST are also included. As can be seen, the trip delay time for high rate-log trip is not calculated for the cases of reactivity insertion rates of 0.001 mk/s and 0.01 mk/s because in these cases it is unlikely that the high rate-log trip would occur even long after the ROP trip occurrence.

The overall comparison between the RFSP-IST determined and POINTSIM calculated trip delay times show good agreement. The largest difference is +55 ms for SDS2 high rate-log trip with the reactivity insertion rate of 1.0 mk/s. It should be noted that larger differences are revealed for the high rate-log trips, which could possibly be attributed to the sensitivity of rate-log interpolations. Furthermore, the RFSP-IST trip delay times are more conservative compared to the POINTSIM results in the case of ROP trips for the reactivity insertion rate ≥ 0.1 mk/s and vice versa for the reactivity insertion rate ≤ 0.01 mk/s. The magnitude of trip delay time differences between the RFSP-IST and POINTSIM results are irrelevant and can be ignored for all practical purposes.

In Table 2, similar results are shown only for the RFSP-IST determined trip times that are obtained with the depleted and undepleted adjuster rod loading. The range of reactivity insertion rate is again 0.001~2.0 mk/s. The differences between the two cases should be ignored for all practical purposes, as in the previous case. The largest difference is +44 ms for SDS2 ROP trip with the reactivity insertion rate of 0.001 mk/s. The effect of isotopic depletion of the stainless steel adjuster rods on the trip delay times would be practically negligible.

Furthermore, it could be observed from Table 2 that the SDS actuation trips occur consistently earlier in the cases of depleted adjuster rod loading, compared to the cases of undepleted adjuster rod

Table 1 RFSP-IST and POINTSIM Trip Delay Time For Initial 100% FP*

Shutdown System	Reactivity Insertion Rate (mk/s)	RFSP-IST SDS Actuation Trip Time (s)	RFSP-IST Trip Delay Time (s)	POINTSIM+ Trip Delay Time (s)	Trip Delay Time Diff. (ms)
sds1-rop	0.001	139.539	2.845	2.882	-37
sds2-rop	0.001	139.545	2.860	2.882	-22
sds1-log	0.001	nc	nc	nc	nc
sds2-log	0.001	nc	nc	nc	nc
sds1-rop	0.01	31.668	0.794	0.810	-16
sds2-rop	0.01	31.667	0.802	0.810	-8
sds1-log	0.01	nc	nc	nc	nc
sds2-log	0.01	nc	nc	nc	nc
sds1-rop	0.1	6.317	0.262	0.260	2
sds2-rop	0.1	6.317	0.266	0.260	6
sds1-log	0.1	24.902	0.597	0.550	47
sds2-log	0.1	33.727	0.548	0.540	8
sds1-rop	1.0	1.159	0.110	0.090	20
sds2-rop	1.0	1.159	0.111	0.090	21
sds1-log	1.0	0.821	0.635	0.650	-15
sds2-log	1.0	1.375	0.635	0.580	55
sds1-rop	2.0	0.713	0.094	0.070	24
sds2-rop	2.0	0.712	0.093	0.070	23
sds1-log	2.0	0.511	0.448	0.450	-2
sds2-log	2.0	0.680	0.556	0.570	-14

* Fresh Core with Depleted Adjuster Rod Loading and 2.747 ppm Boron in Moderator System
+ Data extracted from Reference 3

Table 2 RFSP-IST SDS Actuation Trip Time and Trip Delay Time for Initial 100% FP

Shutdown System	Reactivity Insertion Rate (mk/s)	SDS Actuation TripTime (s)		Trip Delay Time (s)		Trip Delay Time Diff. (ms)
		Depleted ADJ Rod*	Undepleted ADJ Rod+	Depleted ADJ Rod*	Undepleted ADJ Rod+	
sds1-rop	0.001	139.539	139.712	2.845	2.820	25
sds2-rop	0.001	139.545	139.716	2.860	2.816	44
sds1-log	0.001	nc	nc	nc	nc	nc
sds2-log	0.001	nc	nc	nc	nc	nc
sds1-rop	0.01	31.668	31.728	0.794	0.810	-16
sds2-rop	0.01	31.667	31.723	0.802	0.810	-8
sds1-log	0.01	nc	nc	nc	nc	nc
sds2-log	0.01	nc	nc	nc	nc	nc
sds1-rop	0.1	6.317	6.324	0.262	0.262	0
sds2-rop	0.1	6.317	6.325	0.266	0.266	0
sds1-log	0.1	24.902	24.953	0.597	0.573	24
sds2-log	0.1	33.727	33.794	0.548	0.548	0
sds1-rop	1.0	1.159	1.160	0.110	0.111	1
sds2-rop	1.0	1.159	1.160	0.111	0.112	-1
sds1-log	1.0	0.821	0.823	0.635	0.635	0
sds2-log	1.0	1.375	1.380	0.635	0.640	-5
sds1-rop	2.0	0.713	0.713	0.094	0.093	1
sds2-rop	2.0	0.712	0.713	0.093	0.094	-1

sds1-log	2.0	0.511	0.512	0.448	0.448	0
sds2-log	2.0	0.680	0.681	0.556	0.557	-1

*/+ Fresh Core with 2.747 ppm and 2.606 ppm Boron in Moderator System, respectively

loading for the reactivity insertion rate ≤ 0.1 mk/s. In other words, for the same amount of reactivity insertion in time, the fluxes in the core rise faster proportionally with the loading of less parasitic materials during a transient of loss of reactivity control. For transients with stronger reactivity insertion rate, the differences between the SDS actuation trip times with the depleted and undepleted adjuster rod loading become so small that it would not convey any consequential implications.

5. Loss of Regulation Simulations

The simulation of LOR using CATHENA is presented only for one case of 100% FP initial power level based upon the fresh core model loaded with the depleted adjuster rods and with 2.747 ppm boron in the moderator system. The loss of reactivity control is modelled by applying the reactivity insertion rate of 0.001 mk/s. In order to assess the validity of trip delay time and reactivity insertion transient as derived from the results of the RFSP-IST simulations discussed in Sections 3-4, the LOR simulation is also conducted with the POINTSIM calculated trip delay time quoted from Reference 3 (see Table 1).

The trip delay times used in the LOR simulations as obtained from RFSP-IST and POINTSIM are 2.860 s and 2.882 s, respectively. The reactivity transient for the trip delay time of 2.860 s is imported directly from the simulation of *CERBERUS module, and the numerical values of reactivity at each time point during the transient are fed into the CATHENA code, while, for the trip delay time of 2.882 s, a flat reactivity insertion rate of 0.001 mk/s is applied during the entire duration of transient.

The *CERBERUS module generated dynamic reactivity values are plotted in Figure 2 with the exclusion of a few values at the beginning of transient due to irrationality. The slope of the line shown in Figure 2 is 1.00567e-3 mk/s, and it is obtained using least-square fitting. The slope is about a half percent larger compared to the flat rate of 0.001 mk/s.

For the CATHENA simulations, the reactivity effects due to the change of the coolant density, the coolant temperature and the fuel temperature during LOR transients are not accounted for so that it can lead to more isolated observation of the trip delay time effects on the transient behaviour. The simulation results for the assessment of fuel performance using the CATHENA high powered slave channel model (O6) (Ref. 14) are briefly summarized in Table 3; only three parameters of interest are quoted to make judgement on the validity of the procedures developed in the present study to determine trip delay times using RFSP-IST.

The SDS (ROP) actuation trip time occurs 0.82 s earlier with the RFSP-IST determined trip delay time and *CERBERUS module generated LOR reactivity transient compared to the case of the CATHENA input based upon the POINTSIM trip delay time and flat reactivity insertion rate. This is consistent considering the fact that the RFSP-IST trip delay time is 22 ms less than the POINTSIM trip delay time and the *CERBERUS module generated LOR reactivity insertion rate is slightly greater than 0.001 mk/s (see Figure 2 which shows the reactivity transient line least-square fitted slope of 1.00576e-3 mk/s).

Consequently, the peak sheath temperature of the fuel elements reaches 1.02 s earlier for the RFSP-IST trip delay time case compared to the POINTSIM trip delay time case. The differences between the peak sheath temperatures of both cases are very small and practically negligible. The increase of

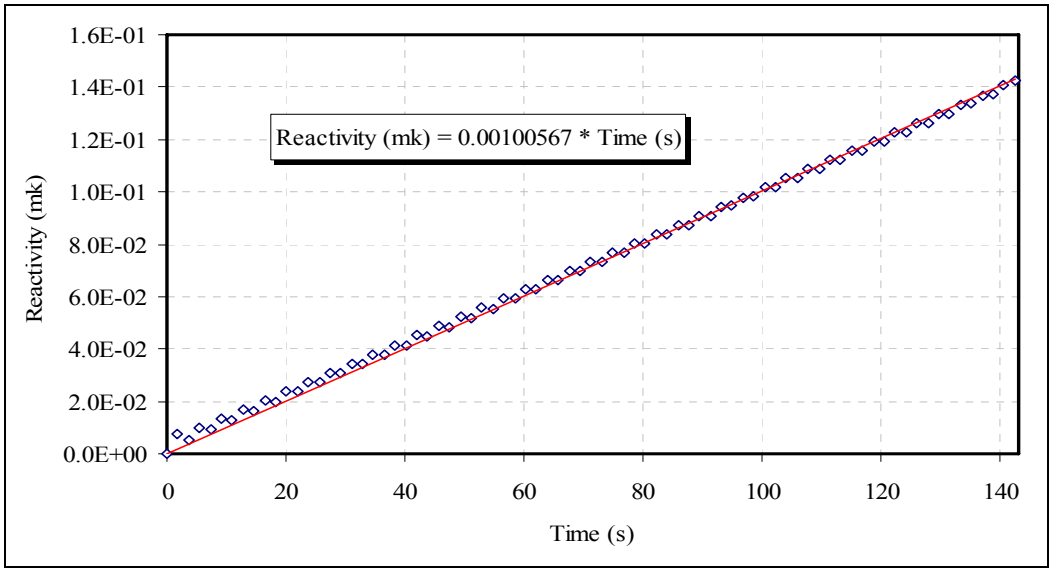

Figure 2 The *CERBERUS Module Generated Dynamic Reactivity Transient

sheath temperature at the peak value is about ~17 ^{o}C from the initial peak sheath temperature of 357.93 ^{o}C. Two cases reveal the same values of peak ROH pressure of 10.349 MPa(a) and normalized peak reactor total power of 1.168. Overall, the results of both cases are in good agreement, such that, using the procedures developed in the present study would not convey any consequential implications to the final outcome of Wolsong-1 LOR safety analyses.

Table 3 CATHENA LOR Simulation Results Based Upon RFSP-IST and POINTSIM Trip Delay Times and Reactivity Transients

Trip Delay Time (s)	SDS (ROP) Actuation Trip Time (s)	Time of Peak Sheath Temperature* (s)	Peak Sheath Temperature* (Deg C)
2.860 (RFSP-IST)	143.841	143.720	375.02
2.882 (POINTSIM)	144.661	144.740	375.03

* High Powered Slave Channel – O6

The maximum sheath temperature transients are graphically shown in Figure 3 for comparison purposes. The relative differences are calculated using the POINTSIM trip delay time based results as references. For convenience, the absolute values of the relative differences are plotted. As expected the relative differences are very small, less than 0.1%, until the SDS (ROP) actuation trip time near around ~144 s (see Table 3), and the maximum sheath temperatures obtained for the RFSP-IST reactivity insertion rate, which is slightly greater than the flat 0.001 mk/s (see Figure 2), are slightly higher than the POINTSIM trip delay time based maximum sheath temperatures until then. After ~144 s the maximum sheath temperatures obtained for the POINTSIM trip delay time based transient are higher than the other case because of the later SDS (ROP) actuation trip time. And the maximum relative difference is about ~-3% at around ~146 s, and the relative differences

remain negative for further duration of the transient after ~146 s and becomes about ~-1% when the maximum sheath temperatures fall down near to ~300 ^{o}C. The relative differences become smaller and finally the maximum sheath temperatures of both cases merge closely to the levelled-off value of ~270 ^{o}C.

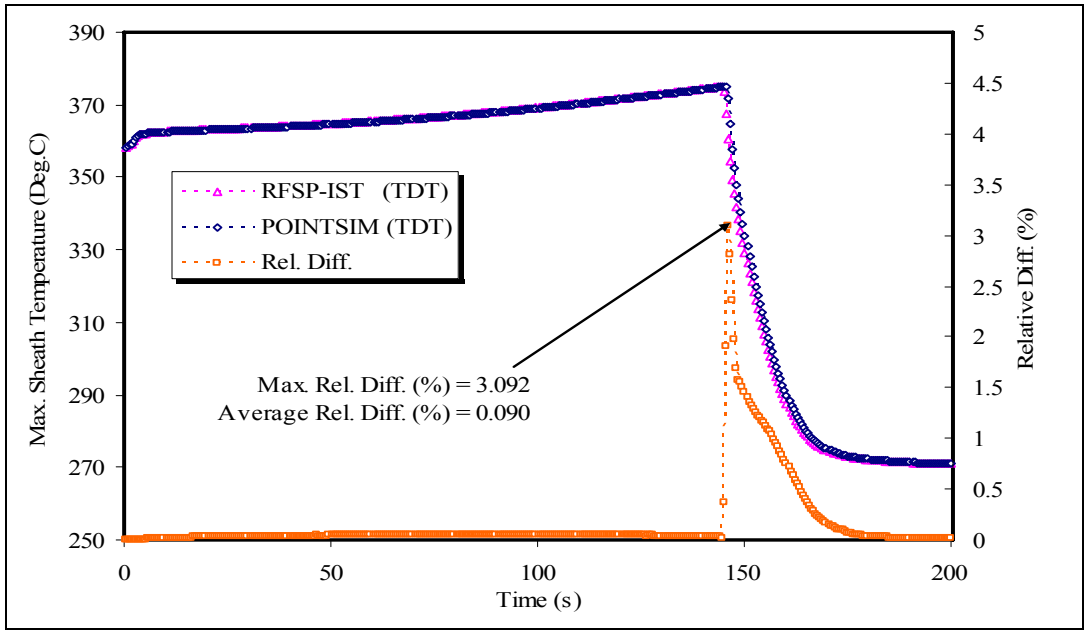

Figure 3 Maximum Sheath Temperature Transients and Relative Differences

6. Conclusions

It can be concluded that the procedures developed in the present paper to determine trip delay times using RFSP-IST could be used in place of the POINTSIM functions for the Wolsong-1 LOR simulations. The CATHENA LOR simulation results using the RFSP-IST determined trip delay time and *CERBERUS module generated reactivity transient confirm clearly that the present methodology would not convey any consequential implications to pose concerns to the quality of LOR safety analyses against the previously practiced methodology, based upon the POINTSIM related code system.

7. Acknowledgements

The authors wish to express their appreciation to Hak-Sung Kim and Hyung-Min Son, ACT Co., Ltd., for the LOR simulations using RFSP-IST and CATHENA, respectively.

8. References

[1] B. Hanna, "CATHENA: A Thermalhydraulic Code for CANDU Analysis", J. Nuclear Engineering and Design, 180, p113-131.

[2] L.C. Choo, “Wolsong 2 Safety Analysis Basis Documentation for Loss of Regulation (Loss of Reactivity Control)”, 86-03500-SAB-013, Rev. 0, AECL, August 1991.

[3] A. Ranger and L.C. Choo, “Trip Coverage Analysis – Loss of Regulation - (Loss of Reactivity Control)”, Wolsong NPP 2/3/4, 86-03500-AR-018, Rev. 1, AECL, 1994 March.

[4] A. Ranger, “Analysis Report – Documentation of POINTSIM.2 Model for Wolsong Trip Coverage Analysis”, Wolsong NPP 2/3/4, 86-03500-AR-007, Rev. 0, AECL, 1992 February.

[5] A. Ranger, “SOPHT Control Model and Data for Wolsong 2 Trip Coverage Analysis”, Analysis Report 86-03500-AR-002, Rev. 0, AECL, December 1991.

[6] B. Rouben, "RFSP-IST, The Industry Standard Tool Computer Program for CANDU Reactor Core Design and Analysis", Proceedings of the 13th Pacific Basin Nuclear Conference, Shenzhen, China, Oct. 21-25, 2002.

[7] D. Altiparmakov, "New Capabilities of the Lattice Code WIMS-AECL", Proc. Int. Conf. on Reactor Physics, Nuclear Power: A Sustainable Resource, PHYSOR-2008, Interlaken, Switzerland, September 14-19, 2008.

[8] T. Liang, W. Shen, E. Varin and K. Ho, “Improvement and Qualification of WIMS Utilities”, 29th Annual CNS Conference, Toronto, June 1 - 4, 2008

[9] M. Dahmani, “Qualification and Development Plan for the T16MAC Version 1.0”, AECL Report 153-113190-PLA-002, Rev. 0, 2007 November.

[10] G. Marleau, A. Hebert, and R. Roy, "A User Guide for DRAGON", Report IGE-174, Rev.5, École Polytechnique de Montréal , April 2000.

[11] Yonghee Kim, Gyuhong Roh, Won-Young Kim, Hak-Sung Kim and Joo-Hwan Park, “A Preliminary Assessmnet of the Adjuster Rod Depletion Effect in the CANDU Reactor”, Transactions of the Korean Nuclear Society Autumn Meeting, PyeongChang, Korea, October 30-31, 2008.

[12] J.V. Donnelly, “Development of a Simple-Cell Model for Performing History-Based RFSP Simulations with WIMS-AECL”, FFC-RCP-005, Technical Report, AECL, 1997 August.

[13] W.H. Press, B.P. Flannery, S.A. Teukolsky and W.T. Vetterling, “Numerical Recipes”, Cambridge University Press, 1986.

[14] B.J. Moon, “CATHENA Fuel Channel Model”, 59RF-03500-AR-009, Rev. 0, KOPEC, August 2008